Cell Metabolism
Article

Bace2 Is a β Cell-Enriched Protease that Regulates Pancreatic β Cell Function and Mass

Daria Esterházy,[1,2] Ina Stützer,[1,2] Haiyan Wang,[3] Markus P. Rechsteiner,[2,4] Jeremy Beauchamp,[3] Heinz Döbeli,[3] Hans Hilpert,[3] Hugues Matile,[3] Michael Prummer,[3] Alexander Schmidt,[1,2] Nora Lieske,[1] Bernhard Boehm,[6] Lorella Marselli,[7] Domenico Bosco,[10] Julie Kerr-Conte,[11] Ruedi Aebersold,[1,2,8] Giatgen Andreia Spinas,[2,5] Holger Moch,[2,4] Cristiano Migliorini,[3] and Markus Stoffel[1,2,9,*]
[1]Institute of Molecular Systems Biology
[2]Competence Centre for Systems Physiology and Metabolic Diseases
ETH Zurich, Zurich 8093, Switzerland
[3]F. Hoffmann-La Roche, Basel 4070, Switzerland
[4]Institute of Surgical Pathology
[5]Division of Endocrinology, Diabetes, and Clinical Nutrition
University Hospital Zurich, Zurich 8091, Switzerland
[6]Division of Endocrinology and Diabetes, Ulm University, Ulm 89070, Germany
[7]Section on Islet Transplantation and Cell Biology, Joslin Diabetes Center, Boston, MA 02215, USA
[8]Faculty of Science
[9]Faculty of Medicine
University of Zurich, Zurich 8091, Switzerland
[10]Cell Isolation and Transplantation Center, University Hospital, Geneva 1121, Switzerland
[11]Department of Surgery, INSERM U859, Lille 2 University, Lille 59045, France
*Correspondence: stoffel@imsb.biol.ethz.ch
DOI 10.1016/j.cmet.2011.06.018

SUMMARY

Decreased β cell mass and function are hallmarks of type 2 diabetes. Here we identified, through a siRNA screen, beta site amyloid precursor protein cleaving enzyme 2 (Bace2) as the sheddase of the proproliferative plasma membrane protein Tmem27 in murine and human β cells. Mice with functionally inactive Bace2 and insulin-resistant mice treated with a newly identified Bace2 inhibitor both display augmented β cell mass and improved control of glucose homeostasis due to increased insulin levels. These results implicate Bace2 in the control of β cell maintenance and provide a rational strategy to inhibit this protease for the expansion of functional pancreatic β cell mass.

INTRODUCTION

Type 2 diabetes is characterized by hyperglycemia resulting from an inability of the endocrine pancreas to secrete sufficient insulin to meet the increased metabolic demands that are associated with insulin resistance (Kahn et al., 2006). Two defects have consistently been reported in patients with type 2 diabetes: gradual deterioration of β cell function and a reduction in pancreatic β cell mass. The molecular mechanisms leading to β cell failure in type 2 diabetes are incompletely understood, but several lines of evidence suggest that mitochondrial dysfunction, oxidative and ER stress, dysfunctional fatty acid metabolism, glucolipotoxicity, and amyloid deposition contribute to β cell demise and ultimately result in functional β cell alterations and loss of β cell mass by apoptosis (Donath and Halban, 2004; Kahn et al., 2006).

The plasma membrane (PM) of pancreatic β cells is a highly specialized compartment regulating a variety of processes pivotal to proper β cell function. Due to its accessibility, the PM is also rich in pharmacological targets such as ion channels, transporters, and growth factor receptors. Many of these cell surface and secreted factors are critically dependent on the activity of proteases, which contribute to autocrine and paracrine shedding of growth factors and their receptors as well as to regulating extracellular matrix turnover. Tmem27 (also termed collectrin), a 46 kDa type I transmembrane protein, is a homolog of the noncatalytic domain of angiotensin-converting enzyme-related carboxypeptidase (Ace2). Its expression has only been reported in the brush border membrane of the proximal tubules and collecting ducts of the kidney (Zhang et al., 2001) and in the pancreatic β cell (Akpinar et al., 2005). Tmem27 was first identified in the kidney by virtue of its upregulation in hypertrophic kidneys after renal ablation (Zhang et al., 2001). In this organ, Tmem27 stabilizes apical amino acid transporters and is essential for amino acid reabsorption (Danilczyk et al., 2006; Malakauskas et al., 2007). In pancreatic islets Tmem27 was initially recognized as one of the most strongly regulated targets of the transcription factor Tcf1 (HNF1α), mutations of which lead to the most common form of maturity onset diabetes of the young (MODY3) (Shih et al., 2001). Functionally, overexpression of Tmem27 in β cells leads to increased proliferation in vitro and increased pancreatic β cell mass in vivo (Akpinar et al., 2005). In another study, overexpression of Tmem27 was reported to augment glucose-stimulated insulin secretion (GSIS) (Fukui et al., 2005). The abundance of Tmem27 protein in β cells is furthermore regulated by ectodomain cleavage, which leads to two cleavage

products, a 25 kDa N-terminal part that is released into the extracellular space (the shed fragment), and a 22 kDa C-terminal fragment (CTF) remaining in the membrane that is rapidly degraded (Akpinar et al., 2005). This shedding process inactivates Tmem27, since neither the shed nor the CTF fragment of Tmem27 had mitogenic activity.

The restricted expression of Tmem27 and its growth-promoting and insulin-stimulatory activity in pancreatic β cells coupled to a mechanism of inactivation in β cells by ectodomain shedding led us to hypothesize that increasing Tmem27 levels by targeting its protease may have beneficial consequences for β cell function and growth. In the experiments described here, the Tmem27 cleavage process served as a readout to identify the Tmem27 sheddase and determine whether genetic or pharmacological inhibition of this protease mimics the effects of Tmem27 overexpression in vivo.

RESULTS

Identification of Bace2 as the Tmem27 Sheddase

To identify the protease that cleaves Tmem27, we performed a 35-compound protease inhibitor screen, in which all major classes of proteases were targeted, and assayed for a decrease in shed Tmem27 from the mouse insulinoma cell line MIN6. Cells were cultured in the presence of the inhibitor or control vehicle, and shed Tmem27 in the supernatant (SN) was measured by immunoblotting. Several compounds of the aspartyl protease inhibitor class showed inhibitory activity (see Figures S1A and S1B available with this article online). We also executed a siRNA screen targeting 29 abundant β cell surface proteases by transfecting MIN6 cells and measuring N-terminal, shed Tmem27 in the SN after 24 hr. The localization of the proteases to the cell surface was confirmed by live cell protein N-glycocapture (Wollscheid et al., 2009) followed by mass spectrometry (MS) (data not shown). Silencing of Bace2 by RNA interference (RNAi) resulted in a marked reduction of Tmem27 in the SN, similar to control transfections in which Tmem27 was silenced (Figure 1A). Inhibition of other proteases had no comparable effect on Tmem27 shedding. Full-length (FL) Tmem27 in the corresponding cell lysates (CLs) was approximately three times higher in cells treated with different siRNAs against Bace2 compared to control cells, indicating that the absence of Bace2 stabilizes Tmem27 (Figure 1B). Tmem27 transcript levels were unaltered upon inactivation of Bace2 by RNAi, demonstrating that Tmem27 stabilization occurred posttranscriptionally (Figure 1C). Since most known substrates of Bace2 are also targets of its homolog Bace1, we also measured Tmem27 levels in cells in which Bace1 was inactivated by RNAi. The amount of Tmem27 in CL and SN was similar in cells treated with Bace1 and control siRNAs (Figure 1D), ruling out any significant contribution of Tmem27 shedding by endogenous Bace1 in MIN6 cells. Furthermore, increased expression of human Bace2 (hBace2) led to enhanced shedding of Tmem27 and decreased levels of the FL protein, but ectopic hBace1 did not affect Tmem27 (Figure 1E), thereby further validating that Tmem27 is regulated by Bace2 but not Bace1. Finally, we asked whether the de novo expression of Bace2 was sufficient to induce Tmem27 cleavage in HEK293 cells, a cell line that expresses neither Bace2 (Figure 1F) nor Tmem27 (Akpinar et al., 2005). Upon coexpression of hTmem27 and hBace2, the shed fragment of hTmem27 appeared in the SN, and FL hTmem27 was destabilized (Figure 1F).

The previously described Bace1/2 substrates are structurally diverse type I transmembrane proteins that are subject to subsequent intramembrane cleavage by the γ-secretase complex (Francis et al., 2002) (Figure 1G). In order to establish the extent to which Tmem27 behaves like a canonical Bace1/2 substrate, we determined whether the CTF of Tmem27, generated by Bace2 cleavage, was also a substrate of the γ-secretase complex. Indeed, incubation of MIN6 cells with increasing concentrations of γ-secretase inhibitor DAPT (Zhao et al., 2008) led to the stabilization of a 22 kDa CTF in the CL (Figure 1H).

Peptides based on the amyloid precursor protein (APP) cleavage sites have previously been used in biochemical assays to evaluate Bace1 inhibitors (Turner et al., 2001). To characterize a Tmem27 sequence that could serve as a Bace2 selective substrate, we mapped the Bace2 cleavage sites. Two complementary approaches were taken, one to identify the N terminus of the CTF, and one to determine the C terminus of the shed fragment of Tmem27. To enrich for the CTF, MIN6 cells overexpressing hTmem27 with a shortened cytosolic tail (hTmem27-Δ171-222-V5) were incubated with DAPT. The 17 kDa CTF was isolated (Figure 2A), digested, and analyzed by MS. Two peptides corresponding to the N terminus of the CTF were identified, starting with F117 (site I) or N119 (site II). These peptides were not detected in a FL hTmem27 control sample (Figure 2B). To map the C terminus of the shed part of Tmem27, the SN of MIN6 cells was collected and its digest subjected to MS. A peptide ending at F125 was detected (site III; Figure 2C) and was highly enriched in the SN when hBace2 was overexpressed in MIN6 cells, indicating that site III is a true Bace2 cleavage site as well. These three Tmem27 cleavage sites (Figure 2D) are relatively conserved among different species (Figure 2E) and resemble described Bace2 sites (Farzan et al., 2000; Hussain et al., 2000, 2001; Kuhn et al., 2007; Turner et al., 2002; Yan et al., 2001), which can be grouped into sites where cleavage occurs between a Leu and an Ala/Asp/Asn residue (Figure 2E, indicated in red) and sites cleaved between Phe and a hydrophobic residue (Figure 2E, indicated in blue). Taken together, these findings demonstrate that Tmem27 expression in MIN6 cells is regulated through ectodomain shedding by Bace2 and subsequent cleavage of the CTF by γ-secretase.

Tissue Distribution and Cellular Localization of Bace2 and Tmem27

Bace2 transcripts have previously been reported in multiple tissues, including the pancreas and kidney, the two main sites of Tmem27 expression (Bennett et al., 2000). To determine the relative abundance of Bace2 mRNA, we assayed for the presence of Bace2 transcripts in 27 mouse organs by real-time PCR. Bace2 mRNA expression was highest in pancreatic islets; was expressed at much lower levels in the pituitary, colon, and ovaries; and was virtually absent from all the other tissues (Figure S2A). In contrast, Bace1 mRNA displayed a much broader tissue distribution. Bace2 transcript levels also correlated with Bace2 protein expression in these tissues (Figure S2B).

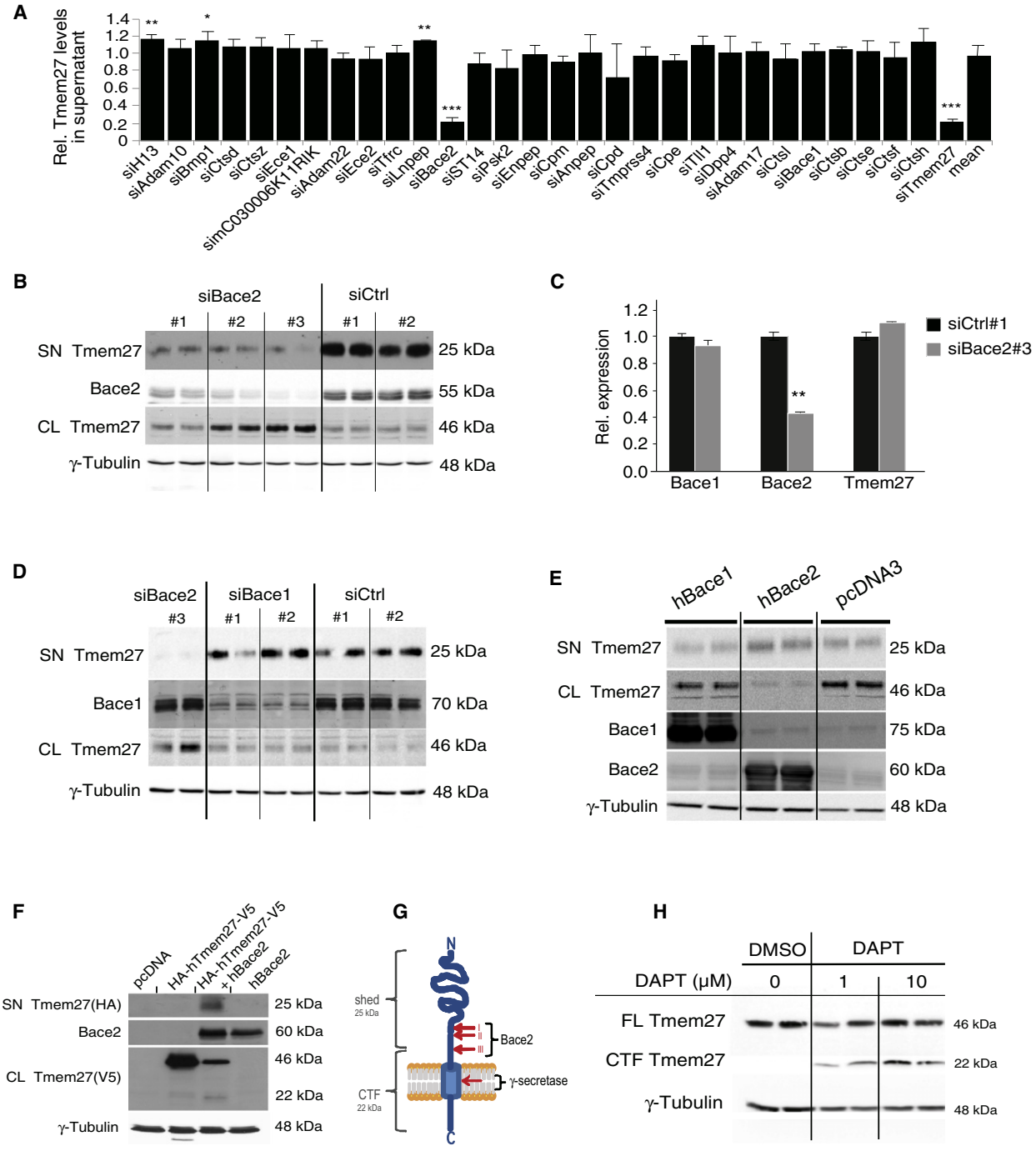

Figure 1. Identification of Bace2 as the Protease Cleaving Tmem27

(A) Quantification of shed Tmem27 in MIN6 supernatant (SN) upon siRNA treatment (n = 4). Signals were normalized to mean screen signal.

(B) Western blot for Tmem27 and Bace2 in MIN6 cell lysate (CL) and SN upon transfection with three different siBace2 (siBace2#1, 2, 3) and control sequences (siCtrl#1, 2). Supernatants were collected for 24 hr starting 12 hr after transfection.

(C) Quantitative PCR analysis of cDNA from MIN6 cells transfected with siBace2 or control siRNA (n = 3).

(D) Western blot for Tmem27 and Bace1 in MIN6 CL and SN upon transfection with two different siBace1 and scrambled control (Ctrl) sequences.

(E) Western blot for Tmem27, Bace1, and Bace2 in MIN6 CL and SN upon transfection with hBace1 or hBace2 expression plasmids.

(F) Immunoblot for Tmem27 in HEK293 CL and SN upon transfection with N-terminally HA-tagged and C-terminally V5-tagged hTmem27 alone or cotransfection with hBace2.

(G) Schematic representation of Tmem27 and its putative cleavage sites by Bace2 and γ-secretase.

(H) Western blot for full-length (FL) Tmem27 and its C-terminal fragment (CTF) in MIN6 CL upon 16 hr treatment with γ-secretase inhibitor DAPT. Data represent means ± SD. *p ≤ 0.05; **p ≤ 0.01; ***p ≤ 0.001.

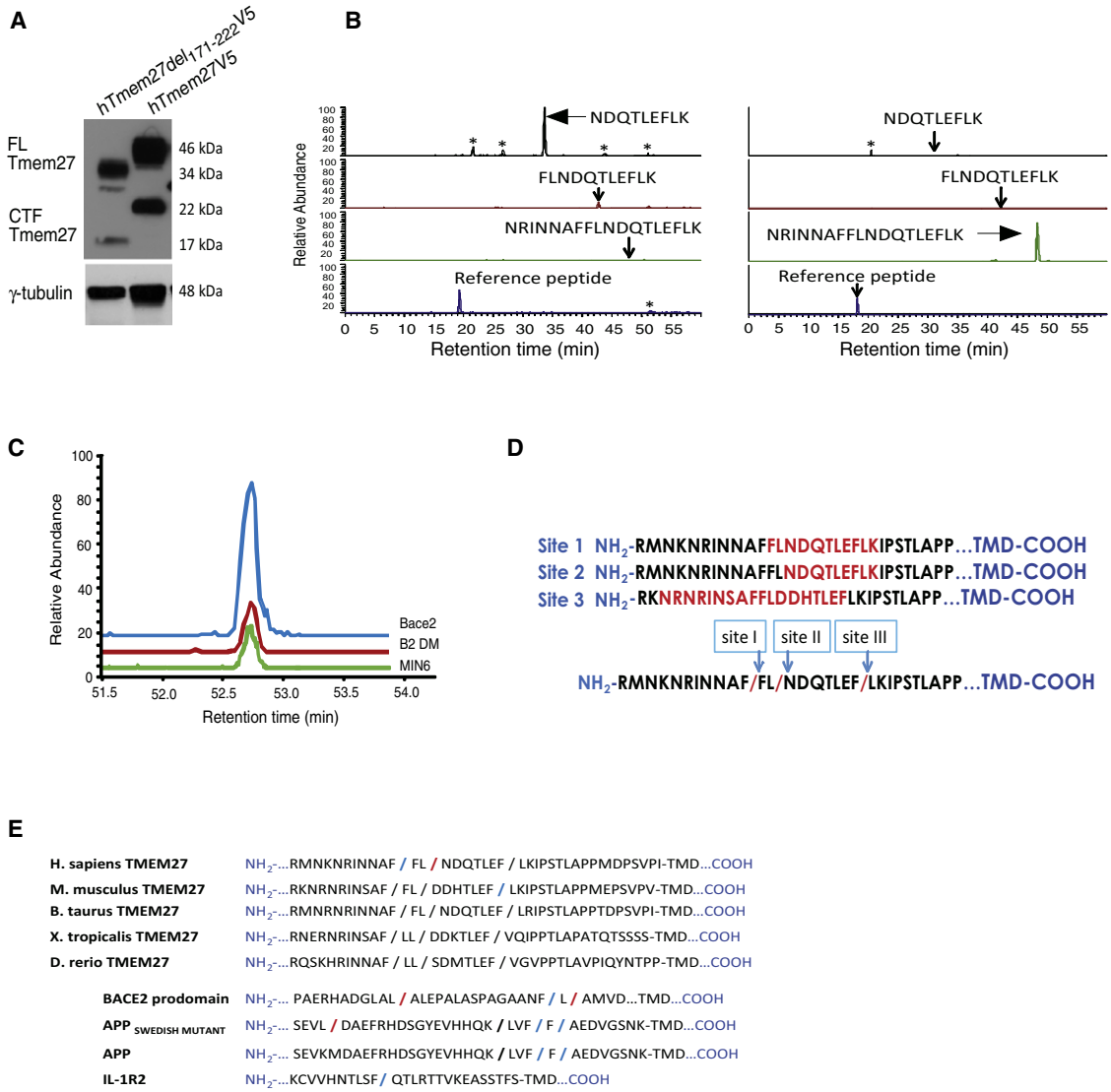

Figure 2. Identification of the Bace2 Cleavage Site in Tmem27

(A) Western blot for Tmem27 in CL from MIN6 expressing either hTmem27Δ171-222-V5 or hTmem27-V5.

(B) Extracted ion chromatograms of Tmem27 peptides found in the Lys-C digest of the hTmem27Δ171-222-V5 CTF (left) and full-length (FL) hTmem27Δ171-222-V5 (right). Asterisks indicate additional spectral peaks.

(C) Extracted ion chromatograms of Tmem27 peptide "INSAFFLDDHTLEF" found in the trypsin digest of the SN from MIN6 cells stably transfected with plasmids pcDNA3 (MIN6), hBace2 (Bace2), or catalytically inactive hBace2 D93A-D303A (B2DM).

(D) Amino acid sequence of the Tmem27 cleavage site region with peptides identified and representing sites I, II, and III highlighted. Note that site III was not seen in the CTF digest because the resulting L126-K127 dipeptide is short and likely lost during sample preparation; the peptides ending at sites I and II could not be observed in the digest of the shed Tmem27 due to the lack of charged residues.

(E) Alignment of the Tmem27 cleavage site region from different species and comparison to other reported Bace2 cleavage sites.

To determine the site of Bace2 presence within the islet, pancreatic sections were costained for Bace2 and insulin, glucagon, somatostatin, and pancreatic polypeptide (PP), as markers for β, α, δ, and PP cells, respectively. In line with recent findings (Finzi et al., 2008), Bace2 signals were solely obtained from insulin-positive cells (Figure 3A). Bace2 appeared to reside mainly in intracellular vesicles that were distinct from insulin granules, as the stainings were nonoverlapping (Figure 3B). To obtain better space resolution, we ectopically expressed hBace2 in MIN6 cells and found the site of localization to be mainly the PM, similar to hTmem27 stainings (Figure 3C). Mouse pancreatic sections were also stained for Bace2 and Tmem27, and the two proteins colocalized (Figure 3D). The site of coexistence was confirmed to be the PM, as both proteins peaked with E-cadherin, a cell surface marker, on a sucrose density gradient (Figure 3E). We also confirmed that Bace2 expression was confined to β cells in humans (Figure S3A). Lastly, to assess if Bace2 and its target Tmem27 are expressed in type 2 diabetic (T2D) patients, we stained pancreatic tissue arrays. In line with a recent report (Altirriba et al., 2010), we found reduced

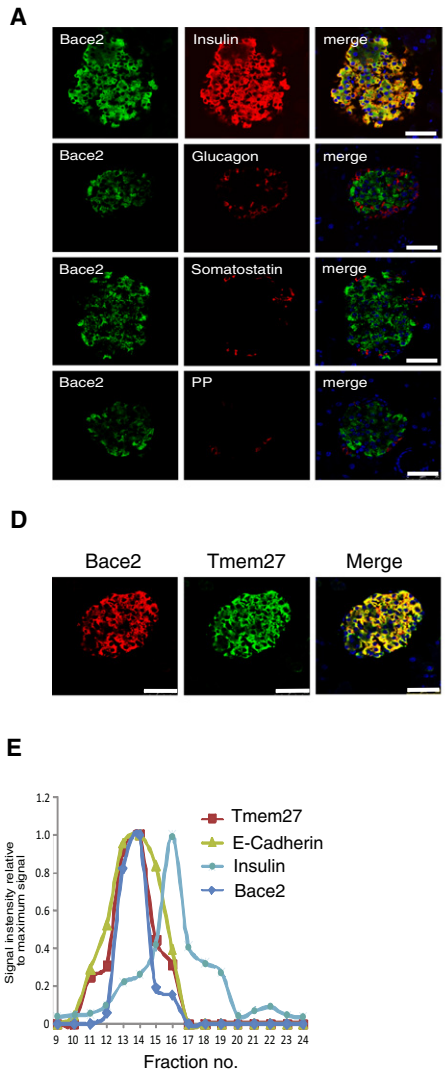

Figure 3. Localization of Bace2 with Respect to Tmem27 in Murine and Human Islets

(A) Immunofluorescence images of murine islets stained for Bace2 and insulin, glucagon, somatostatin, and pancreatic polypeptide (PP). Scale bar, 50 μm.

(B) Image of a murine β cell stained for Bace2 (green) and insulin (red). Scale bar, 10 μm.

(C) 63× immunofluorescence images of MIN6 cells stained for hBace2 (top panel) or hTmem27 (bottom panel) after transfection with either control (pcDNA3) or the respective expression vector.

(D) Image of murine islets stained for Bace2 and Tmem27. Scale bar, 50 μm.

(E) Subcellular fractionation by 10%–70% sucrose gradient ultracentrifugation of MIN6 cells and quantification of β cell proteins by ELISA and immunoblot analysis. Fractions correspond to 2.5% sucrose density increments (fraction 1 = 10%, fraction 24 = 70%).

Tmem27 protein in T2D. Furthermore, no changes in Bace2 expression were observed between control and T2D subjects (Figures S3B–S3D, Table S1). These data indicate that the Bace2/Tmem27 axis is preserved in humans.

Tmem27 Is a Bace2-Specific Substrate in β Cells

To substantiate the evidence that Bace2 is the main protease cleaving Tmem27 in vivo, mice with an in-frame deletion of exon 6 of *Bace2* on both alleles ($Bace2^{\Delta E6/\Delta E6}$) were used for further studies (Dominguez et al., 2005). The deletion of exon 6, which encodes 30 amino acids including the Asp303 residue involved in catalysis, has been predicted to impair the catalytic activity of Bace2 (Dominguez et al., 2005). The inactivity of Bace2ΔE6 was confirmed in MIN6 cells and HEK293 cells, where its overexpression had no effect on Tmem27 levels (Figures S4A and S4B). However, Bace2ΔE6 was still able to bind Tmem27 in a coimmunoprecipitation experiment, but contrary to wild-type Bace2 was unable to destabilize Tmem27 (Figure S4C).

We next compared the levels of shed and FL Tmem27 in the cell culture SN and CLs of size-matched pancreatic islets isolated from $Bace2^{\Delta E6/\Delta E6}$ mice and wild-type littermates. The medium of $Bace2^{\Delta E6/\Delta E6}$ islets after a 24 hr incubation period contained almost no detectable levels of shed Tmem27 compared to the wild-type control media, while FL Tmem27 was greatly enriched in CL of $Bace2^{\Delta E6/\Delta E6}$ islets (Figure 4A). To unambiguously exclude the possibility that Bace1 participates in Tmem27 processing, the same experiment was performed with islets of $Bace1^{-/-}$ mice and wild-type littermates. Intriguingly, the Tmem27 levels in $Bace1^{-/-}$ islet lysates were augmented compared to wild-type lysates (Figure 4B). However, because the Tmem27 ectodomain in the SN was equally elevated, while the Bace2 levels were unchanged, this increase of Tmem27 appeared to be independent of direct cleavage. Finally, cleavage of overexpressed Tmem27 by kidney cells has recently been reported (Altirriba et al., 2010). To test if Bace2 or Bace1 affected kidney Tmem27 cleavage, we measured FL Tmem27 levels in fresh kidney extracts from $Bace2^{\Delta E6/\Delta E6}$ or Bace1 null mice and wild-type littermates. Kidney Tmem27 levels were similar in $Bace2^{\Delta E6/\Delta E6}$ or $Bace1^{-/-}$ and control mice (Figures 4C and 4D), a finding that is consistent with the absence of Bace2 protein in the kidney (Figures S2A and S2B) and the lack of endogenous Tmem27 cleavage from dispersed kidneys (Akpinar et al., 2005). Together, these results demonstrate that Bace2 is the main protease cleaving Tmem27 in primary pancreatic β cells.

$Bace2^{\Delta E6/\Delta E6}$ Mice Exhibit Reduced Blood Glucose Levels, Improved Intraperitoneal Glucose Tolerance, and Increased β Cell Mass

Overexpression of Tmem27 in the β cell leads to β cell expansion and improved glucose homeostasis (Akpinar et al., 2005; Fukui

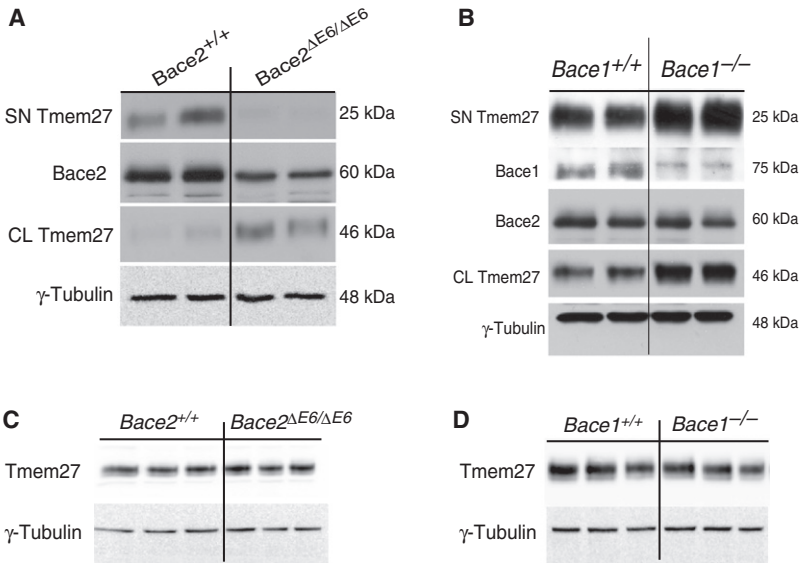

Figure 4. Identification of Bace2 as the Tmem27 Sheddase in Primary β Cells

(A) Western blot for Tmem27 and Bace2 in CL and SN of 100 isolated islets per lane from 15-week-old *Bace2*$^{\Delta E6/\Delta E6}$ mice and *Bace2*$^{+/+}$ littermates.

(B) Western blot for Tmem27, Bace1, and Bace2 in CL and SN of 100 isolated islets per lane from 15-week-old *Bace1*$^{-/-}$ mice and *Bace1*$^{+/+}$ littermates. All islets were incubated in Opti-MEM for 48 hr.

(C) Immunoblot for Tmem27 and γ-tubulin in fresh kidney protein extracts from 15-week-old *Bace2*$^{\Delta E6/\Delta E6}$ and *Bace2*$^{+/+}$ littermates.

(D) Western blot analysis of Tmem27 and γ-tubulin in fresh kidney protein extracts of 15-week-old *Bace1*$^{-/-}$ mice and *Bace1*$^{+/+}$ littermates.

et al., 2005). We therefore investigated if the absence of active Bace2 leads to measurable changes in metabolism. Plasma glucose levels of ad libitum-fed *Bace2*$^{\Delta E6/\Delta E6}$ mice and wild-type littermate controls were monitored up to the age of 16 weeks. No differences in body weight were measured in the two genotypes (Figure 5A), yet *Bace2*$^{\Delta E6/\Delta E6}$ animals displayed persistently reduced blood glucose levels from the age of about 8 weeks on (Figure 5B). To study if *Bace2*$^{\Delta E6/\Delta E6}$ animals exhibited improved performance in a hyperglycemic setting, the two groups were challenged with an intraperitoneal (i.p.) glucose tolerance test (IPGTT). *Bace2*$^{\Delta E6/\Delta E6}$ mice displayed lower blood glucose levels in the fasted state and during the IPGTT compared to wild-type mice (Figure 5C), indicating that these mice clear glucose from the circulation more efficiently. Plasma insulin levels after a 6 hr fast and 15 min after a glucose injection were increased in *Bace2*$^{\Delta E6/\Delta E6}$ compared to control mice (Figure 5D), while fasting glucagon levels remained unaltered (33.9 ± 4.3 pg/ml and 30.3 ± 4.7 pg/ml in *Bace2*$^{\Delta E6/\Delta E6}$ and wild-type mice, respectively). Furthermore, isolated *Bace2*$^{\Delta E6/\Delta E6}$ islets secreted more insulin when exposed to glucose for 30 min in a glucose stimulated insulin secretion assay (GSIS) than did size-matched islets from wild-type mice (Figure 5E), demonstrating that the improved glucose tolerance was in part explained by an increased insulin secretory capacity of *Bace2*$^{\Delta E6/\Delta E6}$ islets. Increased insulin sensitivity of *Bace2*$^{\Delta E6/\Delta E6}$ mice was ruled out by an insulin tolerance test (ITT), in which mutant and control animals behaved similarly (Figure 5F).

In order to test if inactivation of Bace2 also has an effect on pancreatic β cell growth, we measured the β cell mass and total pancreatic insulin content in 20-week-old *Bace2*$^{\Delta E6/\Delta E6}$ and control mice. The pancreatic β cell mass increased approximately 30% in pancreata of *Bace2*$^{\Delta E6/\Delta E6}$ animals compared to wild-type littermates (Figure 5G), as did the pancreatic insulin content (Figure 5H). In contrast, no changes were measured for α cell mass (Figure 5I), as well as δ and PP cell mass (data not shown). To establish whether the increased β cell mass was due to accelerated β cell proliferation, the percentage of cells expressing Ki67, a proliferation marker, was determined (Figure 5J). Since *Bace2*$^{\Delta E6/\Delta E6}$ mice had approximately twice as many Ki67-positive β cells and no apoptosis was observed in the islets (data not shown), the increase in β cell mass is most likely due to an increase in β cell proliferation. Finally, to assess if this proliferative effect of genetic Bace2 inactivation was cell autonomous, the EdU incorporation into insulin-positive cells within dispersed islets (Parnaud et al., 2008) from *Bace2*$^{\Delta E6/\Delta E6}$ and wild-type littermate was determined and found to be increased 1.5-fold (Figure 5K). Taken together, *Bace2*$^{\Delta E6/\Delta E6}$ mice exhibit improved glucose homeostasis that correlates with increased insulin secretory capacity of islets and augmented β cell proliferation and mass. Therefore, the metabolic phenotype of *Bace2*$^{\Delta E6/\Delta E6}$ mice demonstrates that inactivation of Bace2 is beneficial for β cell function.

Identification and Characterization of a Bace2 Inhibitor

To further corroborate the role of Bace2 in vitro and in vivo, the effective inhibitory concentrations (IC_{50}) of five structurally diverse Bace inhibitors, compounds A, B, C, D, and J, toward Bace1, Bace2, and the related aspartyl protease CathepsinD (CTSD) were determined in a Tmem27 and APP cleavage site sequence-based FRET assay (Table S2). Using FRET peptides QTLEFLKIPS and SEIDLMVLDR, corresponding to the hTmem27 cleavage site III (Figure 2E) and the APP cleavage site, respectively, compound J (CpdJ) was superior over compounds A, B, C, and D in terms of potency of Bace2 inhibition and selectivity over CTSD (Table S2). Of note, compound D has recently been described as a Bace2 inhibitor in the pancreatic β cell (Bettegazzi et al., 2010), yet no activity toward Bace1 or Bace2 was observed in our assay. All compounds except compound D inhibited Tmem27 shedding in MIN6 cells and resulted in the stabilization of this substrate in vitro, and none except compound D induced apoptosis, as measured by active caspase-3 immunoblotting (Figures S5A and S5B). Interestingly, treatment with effective Bace2 inhibitors led to the appearance of a higher molecular band in immunoblots, demonstrating that they blocked the autocatalytic prodomain cleavage that is essential for the conversion of the Bace2 zymogen to fully active, mature form and indicative of Bace2 targeting. On the basis of the superior activity and selectivity for Bace2 as well as favorable in vivo pharmacokinetic (PK) properties (data not shown), CpdJ was chosen for further evaluation.

To determine the extent to which the CpdJ-induced stabilization of Tmem27 was dependent on Bace2, we studied the effect of CpdJ in primary islets of wild-type and *Bace2*$^{\Delta E6/\Delta E6}$ animals by western blotting. Wild-type islets treated with CpdJ exhibited a substantial loss of Tmem27 ectodomain-shedding activity and stabilization of FL Tmem27 in the CL (Figure 6A). In contrast, no further changes of shed Tmem27 or FL Tmem27 in total CL were observed upon CpdJ treatment of *Bace2*$^{\Delta E6/\Delta E6}$ islets. Furthermore, CpdJ did not induce a Bace2 prodomain shift in these islets, indicating that Bace2ΔE6 is not a target for CpdJ (Figure 6A). Finally, to study the effect of CpdJ on Tmem27 levels and Bace2 inactivation in a time-dependent manner in vitro, we incubated isolated mouse islets with CpdJ for up to 72 hr and measured Tmem27 stabilization. Tmem27 levels and Bace2 in its zymogen form increased already after 4 hr and continued to rise with prolonged CpdJ incubation (Figure 6B) with no signs of β cell death (data not shown). Together, these data indicated that CpdJ is a potent inhibitor of Bace2 activity in primary β cells in vitro.

We next tested if CpdJ displayed some of the anticipated features of Bace2 inhibition in β cells. The biological consequence of Tmem27 stabilization as a result of Bace2 inhibition by CpdJ was first studied in proliferation assays. MIN6 cells were grown in the absence and presence of CpdJ, and proliferation was measured by following EdU incorporation. The proliferation of MIN6 cells increased upon CpdJ compared to vehicle-treated cells (Figure 6C), and a similar increase in proliferation was measured when Bace2, but not Bace1, was inhibited by RNAi. The proliferation was reduced in CpdJ-treated MIN6 cells in which Tmem27 was silenced, suggesting that the effect of altered Bace2 levels is at least partly dependent on Tmem27 expression (Figure 6C). Conversely, overexpression of Bace2 but not Bace1 led to decreased EdU incorporation that was reversible by the addition of CpdJ (Figure 6D). The levels of Tmem27, Bace1, and Bace2 under all these conditions were analyzed by western blot and revealed a robust correlation between Bace2 levels and proliferation unless Tmem27 was silenced (Figures 6E and 1E). To establish whether the proliferative effect of CpdJ and its dependence on Tmem27 expression also held true in primary cells, murine islets were dispersed and infected with a lentivirus expressing a nontargeting short hairpin (shScramble) or a hairpin targeting Tmem27 (shTmem27). CpdJ or DMSO was added 24 hr later, and the EdU incorporation into insulin-positive cells was determined after further 48 hr. While CpdJ led to increased proliferation in the control infected β cells, the decreased proliferation observed in the cells infected with the Tmem27 targeting virus could not be reversed by CpdJ incubation (Figure 6F). The efficiency of RNAi and CpdJ was confirmed by western blot (Figures S5C and S5D). Lastly, to study the extent to which the proliferative effect of CpdJ was dependent on Bace2, we dispersed *Bace2*$^{\Delta E6/\Delta E6}$ islets and incubated them with CpdJ. In line with the lack of further Tmem27 stabilization or Bace2 zymogen induction upon CpdJ incubation in these islets (Figure 6A), no further increase in proliferation was observed in *Bace2*$^{\Delta E6/\Delta E6}$ islets (Figure S5E). These findings demonstrate that CpdJ is an effective Bace2 inhibitor that exhibits proproliferative activity in vitro that is at least partially dependent on Tmem27 expression.

To investigate if Bace2 inhibition has an acute effect on pancreatic β cell function, we measured GSIS in primary mouse islets. Isolated islets were incubated with CpdJ for 8 hr prior to and during stimulation with increasing concentrations of glucose. No changes in GSIS were measured in islets treated with CpdJ compared to controls (Figure 6G), despite efficient Bace2 inhibition and increased Tmem27 levels after 8 hr (Figure 6B). Even when islets were subjected to GSIS upon CpdJ incubation after 24, 48, and 72 hr, no differences were observed (data not shown). The independence of GSIS on short-term Bace2 inhibition or Tmem27 levels was furthermore supported by the fact that no difference in glucose or L-Arginine response was observed when dispersed islets were infected with shTmem27- or shScramble-expressing lentivirus and incubated in the presence of CpdJ or DMSO prior to the assay (Figure S5F). These data suggest that CpdJ does not act as an acute insulin secretagogue.

Finally, we also tested if CpdJ exhibited proliferative and functional effects in human pancreatic islets. Addition of CpdJ to the culture medium of human islets led to the stabilization of FL Tmem27 and the anticipated Bace2 prodomain shift (Figure 6H). Although differentiated human β cells are thought to be slowly to not proliferating and rather resistant to mitogenic stimuli in cell culture (Efrat, 2008; Parnaud et al., 2008), we assessed the effect of CpdJ on EdU incorporation into mature human β cells (i.e., cells with insulin-positive staining) from a 13- and a 60-year-old female donor (donors A and B respectively). In donor A, 0.5% of the β cells within the dispersed islets were EdU positive after a 60 hr incubation period, while proliferation of β cells from donor B was an even rarer event (0.04% or 1 in 2500 β cells). The addition of 100 nM CpdJ had no significant effect on the proliferation of β cells from either donor, although an overall tendency toward more proliferation was perceived (Figure S5G). Similarly, but in contrast to murine islets, human islets from the same donors displayed the propensity to secrete more insulin upon glucose stimulation when treated with CpdJ for 20 hr prior to and during the assay (Figure S5H).

Taken together, CpdJ had similar biochemical and functional effects on murine β cells in vitro as genetic Bace2 inactivation in vivo: FL Tmem27 was stabilized, β cell proliferation was stimulated, and insulin secretion was not affected after a short time period, analogous to the lack of change in glucose levels in *Bace2*$^{\Delta E6/\Delta E6}$ mice up to the age of 7 weeks. Isolated human islets were more resistant to the proliferative effect of CpdJ but potentially more sensitive to the insulin secretory effect.

Pharmacological Inhibition of Bace2 Increases β Cell Mass and Improves Glycemic Control in *ob/ob* Mice

We next investigated if daily intraperitoneal (i.p.) injection of CpdJ would result in effective inhibition of Bace2 activity in vivo and would therefore be suitable for metabolic studies. Initial PK studies showed that CpdJ was rapidly cleared from the circulation, with a $t_{1/2}$ of 2 hr (Figure S5I). Nonetheless, wild-type mice were treated with a single dose of either 30 or 100 mg/kg, and Tmem27 stabilization and Bace2 prodomain shift were assayed as readouts for Bace2 inhibition 24 hr later. A dose-dependent stabilization of Tmem27 was measured in islet CL, and a Bace2 prodomain shift was detected (Figure S5J), demonstrating that the bioavailability of CpdJ was adequate to

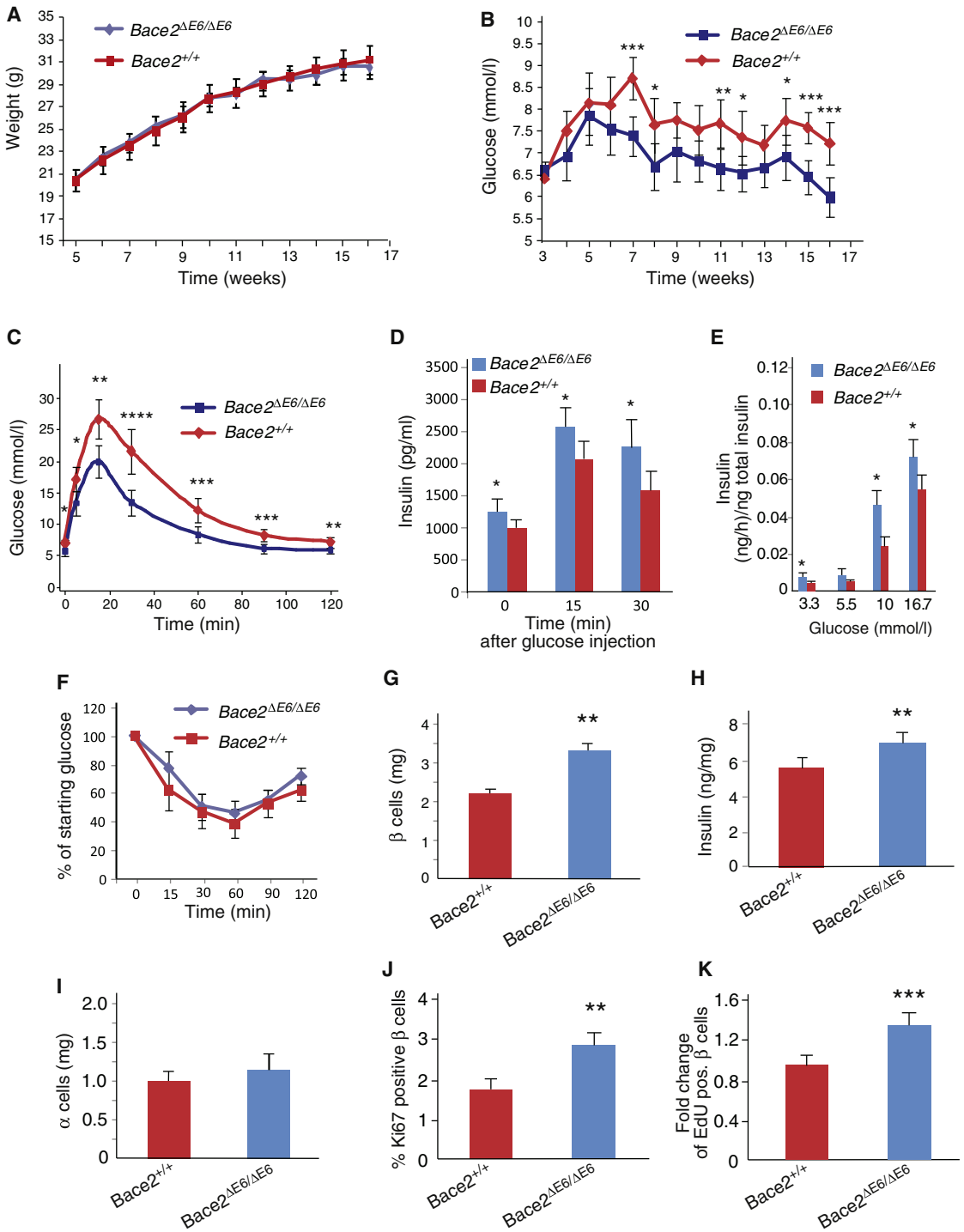

Figure 5. Improved Blood Glucose Homeostasis and Increased β Cell Mass in *Bace2*$^{\Delta E6/\Delta E6}$ Mice

(A) Weight of *Bace2*$^{\Delta E6/\Delta E6}$ and *Bace2*$^{+/+}$ littermate mice (n = 8–10).

(B) Ad libitum-fed blood glucose levels of *Bace2*$^{\Delta E6/\Delta E6}$ and *Bace2*$^{+/+}$ mice (n = 10–12).

(C) Blood glucose levels before (0 min) and after an i.p. glucose injection of 15-week-old *Bace2*$^{\Delta E6/\Delta E6}$ and *Bace2*$^{+/+}$ mice (n = 8–10).

(D) Serum insulin levels of 15-week-old *Bace2*$^{\Delta E6/\Delta E6}$ and *Bace2*$^{+/+}$ mice after a 6 hr fast (0 min) and after an intraperitoneal (i.p.) glucose injection (n = 12).

(E) Insulin released by isolated islets from 15-week-old *Bace2*$^{\Delta E6/\Delta E6}$ and *Bace2*$^{+/+}$ mice incubated at indicated glucose concentrations (n = 3). Insulin secreted was normalized to total insulin content of secreting islets. This result was confirmed in two further independent experiments (data not shown).

(F) ITT of 15-week-old *Bace2*$^{\Delta E6/\Delta E6}$ and *Bace2*$^{+/+}$ mice using 0.5 U insulin/kg body weight (n = 12).

(G) β cell mass of 20-week-old *Bace2*$^{\Delta E6/\Delta E6}$ and *Bace2*$^{+/+}$ mice (n = 3). Mass was calculated by multiplying the fraction of β cell-positive surface area by pancreatic wet weight.

determine the metabolic effect of pharmacological Bace2 inhibition of CpdJ in vivo. Toxicity of the compound was excluded, since the serum levels of alanine transaminase and aspartate transaminase during a 5 day treatment with either dose and a 21 day treatment with 30 mg/kg CpdJ were unaltered compared to vehicle treatment (data not shown).

We then sought to determine if administration of CpdJ could improve glucose tolerance in a mouse model of obesity-related insulin resistance, the *ob/ob* mice. CpdJ led to stabilization of Tmem27 and to the Bace2 prodomain shift already 6 hr after administration and up to 24 hr postadministration (Figure 7A), indicating that a daily dose of 30 mg/kg body weight was sufficient to reach constant Bace2 inhibition. This dose was well tolerated and in contrast to the 100 mg/kg dose affected neither body weight nor food intake (Figure 7B, data not shown). The compound was administered for 21 days in 5-week-old *ob/ob* mice with an IPGTT and an ITT performed at day 11 and 15, respectively. Short-term fasting blood glucose levels started to decrease after 1 week of treatment in CpdJ-treated mice compared to vehicle-receiving controls (Figure 7C). Overnight fasting blood glucose levels were also decreased at day 11 (Figure 7D). The glucose clearance from the blood in CpdJ-treated mice was improved compared to vehicle-treated animals during an IPGTT (Figure 7D). Notably, plasma insulin levels during the IPGTT were increased in CpdJ-treated mice at 15 and 30 min compared to control-treated mice (Figure 7E). The ITT at day 15 revealed no differences in the vehicle- versus CpdJ-treated group, thereby demonstrating that CpdJ does not alter insulin sensitivity (Figure 7F).

We next analyzed the effect of CpdJ on pancreatic β cell mass by performing a morphometric analysis of CpdJ- and vehicle-treated *ob/ob* mice after 21 days of treatment. The pancreatic β cell mass in the CpdJ-treated group was larger than in the vehicle-administered controls (Figure 7G), while the pancreatic α cell mass was not changed (1.00 mg ± 0.13 and 1.04 mg ± 0.27 for vehicle- and CpdJ-treated groups, respectively). Immunostaining of insulin-positive cells with anti-Ki67 antibody revealed an increase in the number of Ki67-positive β cells in the CpdJ-treated group compared to controls (Figure 7H), whereas no apoptosis was observed (data not shown). Finally, to assess if this proliferation effect was islet autonomous, EdU incorporation into nuclei of insulin-positive cells in dispersed *ob/ob* islets was analyzed upon CpdJ treatment compared to DMSO treatment and was found to be elevated 2-fold (Figure 7I). While an 18 day treatment with CpdJ of wild-type mice had no effect on glucose levels (data not shown), similar findings were observed when C57BKS$^{db/db}$ mice, which are known to have more severe insulin secretion defects than *ob/ob* mice (Han et al., 2007; Roe et al., 1994; Winzell et al., 2009), were subjected to the same treatment regime (Figures S6A–S6H), suggesting that the effects of CpdJ were not limited to the *ob/ob* model. Together, our data demonstrate that CpdJ improves glycemic control by increasing functional β cell mass in vivo.

DISCUSSION

In this study, we have identified Bace2 as one of the few membrane proteases reported to be involved in the regulation of pancreatic β cell mass and function. This is at the same time the assignment of a biological function for Bace2.

Tmem27 is a Bace2-specific target, as the other known Bace2 substrates are also cleaved by Bace1, although frequently at a different site. The fidelity of Tmem27 toward Bace2 rather than Bace1 might in part be explained by the enrichment of hydrophobic moieties in the cleavage site that has been found in other Bace2 substrates and distinctively in domains in which Bace1 did not cleave those proteins (Fluhrer et al., 2002; Grüninger-Leitch et al., 2002; Sun et al., 2006; Yan et al., 2001). Another way by which the specificity of interaction of Tmem27 with Bace2 rather than Bace1 could be conferred is by differential compartmentalization: Bace1 is known to be resident primarily in the Golgi-TGN compartments (Gandhi et al., 2004), while Bace2 is localized to the endosomal compartments (Fluhrer et al., 2002; Walter, 2006) and active at less acidic pH than Bace1 (Kim et al., 2002).

The merits of inhibiting Bace2 were discovered in the quest for a protease cleaving Tmem27. Since both overexpression of Tmem27 (Akpinar et al., 2005; Fukui et al., 2005) and ablation of Bace2 activity led to raised Tmem27 protein levels and each setting increases β cell mass and function, it is likely that part of these effects of inactivating Bace2 are mediated by Tmem27. This notion is underpinned by a partial dependency of the action of CpdJ on Tmem27 expression in its ability to stimulate murine β cell proliferation. We did not observe such a dependency of GSIS on Tmem27, consistent with the unaltered insulin secretion from Tmem27 knockout islets (Malakauskas et al., 2009). However, since only generic readouts for β cell function, proliferation, and insulin secretion have been used to measure Tmem27 activity, it is likely that Tmem27 primarily acts upstream of both processes. Given its location at the interface of the intra- and extracellular β cell environment, Tmem27 could possibly act as a sensor (Zhang et al., 2007) or, in analogy to other γ-secretase targets, as a scaffolding protein regulating the plasticity of extracellular matrix and growth hormone signaling (Cavallaro and Dejana, 2011). It is also important to stress that Tmem27 represents only one of likely many and yet-to-be-identified Bace2 β cell targets. This is supported by a recent study, which reported the identification of about 60 Bace targets in HEK293 cells, including known positive regulators of β cell growth such as hepatocyte growth factor receptor (Hemming et al., 2009). Therefore, it is to be expected that a combination of PM Bace2 substrates will

(H) Total insulin content of pancreata from 20-week-old *Bace2*$^{\Delta E6/\Delta E6}$ and *Bace2*$^{+/+}$ mice (n = 5–7).
(I) α-cell mass of *Bace2*$^{\Delta E6/\Delta E6}$ and *Bace2*$^{+/+}$ mice (n = 3).
(J) Percentage of Ki67-positive β cell nuclei in *Bace2*$^{\Delta E6/\Delta E6}$ and *Bace2*$^{+/+}$ pancreata from 7-week-old mice (n = 5).
(K) Fold change of EdU-positive β cells in dispersed *Bace2*$^{\Delta E6/\Delta E6}$ islets compared to *Bace2*$^{+/+}$ islets after 60 hr incubation in presence of 10 μM EdU (n = 4). Islets from four 12-week-old mice per genotype were analyzed, and at least 3000 β cells were counted per animal. Percentage of EdU-positive cells was 2.5%–4%. Data shown in (A)–(C) and (F)–(I) came from the same cohort of animals. (D), (E), (J), and (K) each came from a separate set of animals. Data represent means ± SD. $^{*}p \leq 0.05$; $^{**}p \leq 0.01$; $^{***}p \leq 0.001$.

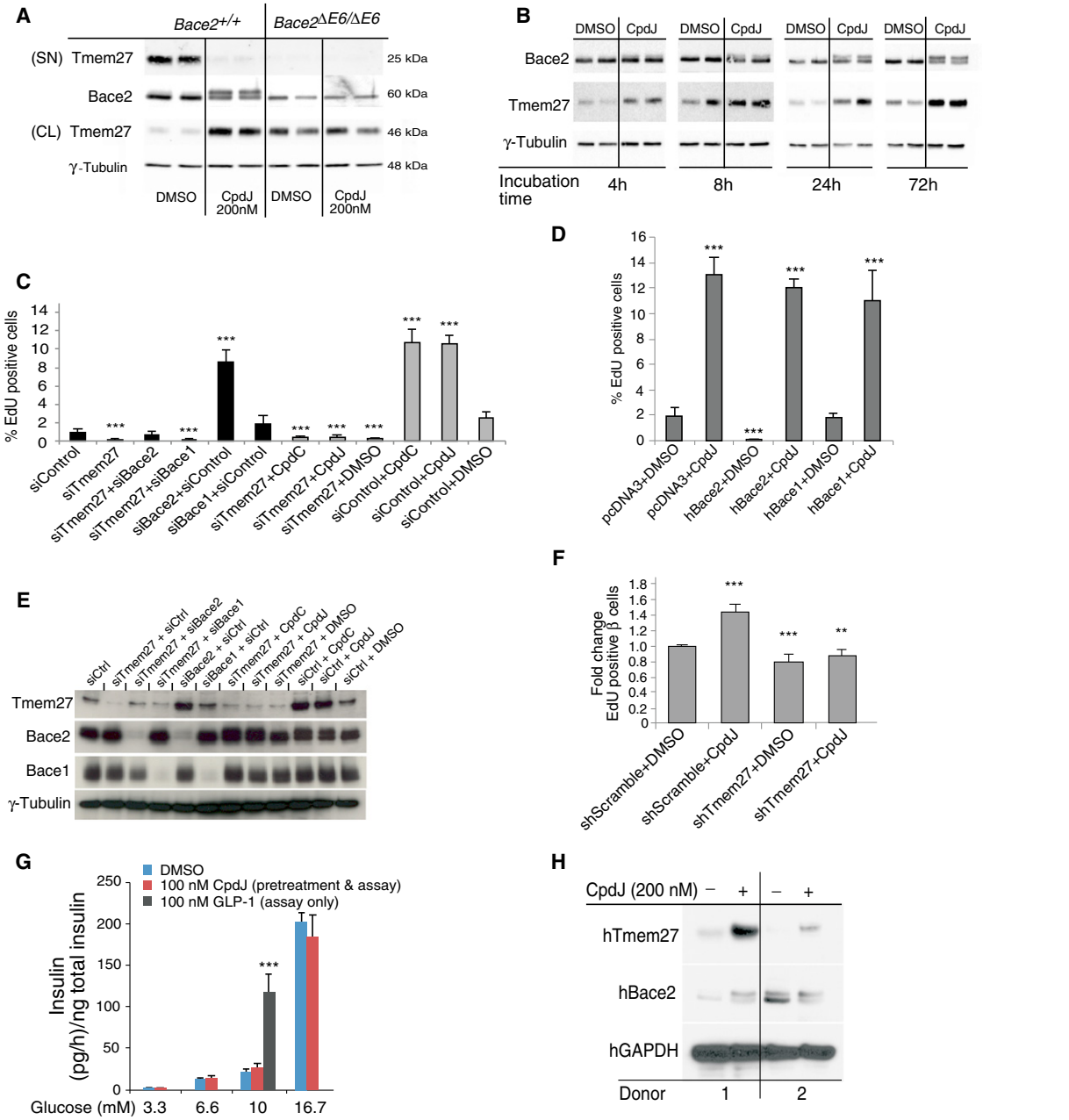

Figure 6. Pharmacological Inhibition of Bace2 and Its Effects on MIN6 Proliferation, Insulin Secretion, and Tmem27 and Bace2 Levels in Isolated Islets

(A) Immunoblot of Tmem27 and Bace2 in SN and CL of isolated islets from 12-week-old *Bace2*$^{\Delta E6/\Delta E6}$ and wild-type littermate control mice treated with 200 nM CpdJ or DMSO for 48 hr. Note additional higher molecular weight band of Bace2 in wild-type lanes upon treatment with inhibitor, reflecting the Bace2 prodomain shift occurring upon Bace2 inhibition.

(B) Western blot for Tmem27 and Bace2 in CL of isolated islets from 8-week-old mice treated with 100 nM CpdJ or DMSO after indicated incubation time.

(C and D) Quantification of EdU incorporation (expressed as percentage of EdU-positive nuclei over total nuclei) of MIN6 cells upon treatment with 100 pmol of siRNA (C) or 1 μg plasmid/ 10^6 cells (D) and 100 nM CpdJ or DMSO. On average, 7000 MIN6 nuclei were assessed per well. The experiment was done in three independent repeats, 30 wells per group in total. All pairwise comparisons with the untreated group were highly significant (binomial linear mixed-effect model with post hoc correction, $p < 10^{-16}$).

(E) Western blot for Tmem27, Bace1, and Bace2 in MIN6 CL after treatment with 100 pmol of siRNA and 100 nM CpdJ or DMSO.

(F) Fold change of EdU-positive β cells in dispersed islets from 4-week-old C57Bl6 mice infected with lentivirus expressing hairpin against Tmem27 (shTmem27) compared to nontargeting hairpin (shScramble) (n = 4). Dispersed islets were incubated in the presence of 100 nM CpdJ or DMSO, which was added together with EdU 24 hr postinfection, and cells were fixed 72 hr posttransfection. At least 3000 β cells were counted per animal. Percentage of EdU-positive and insulin positive cells was 4%–7%.

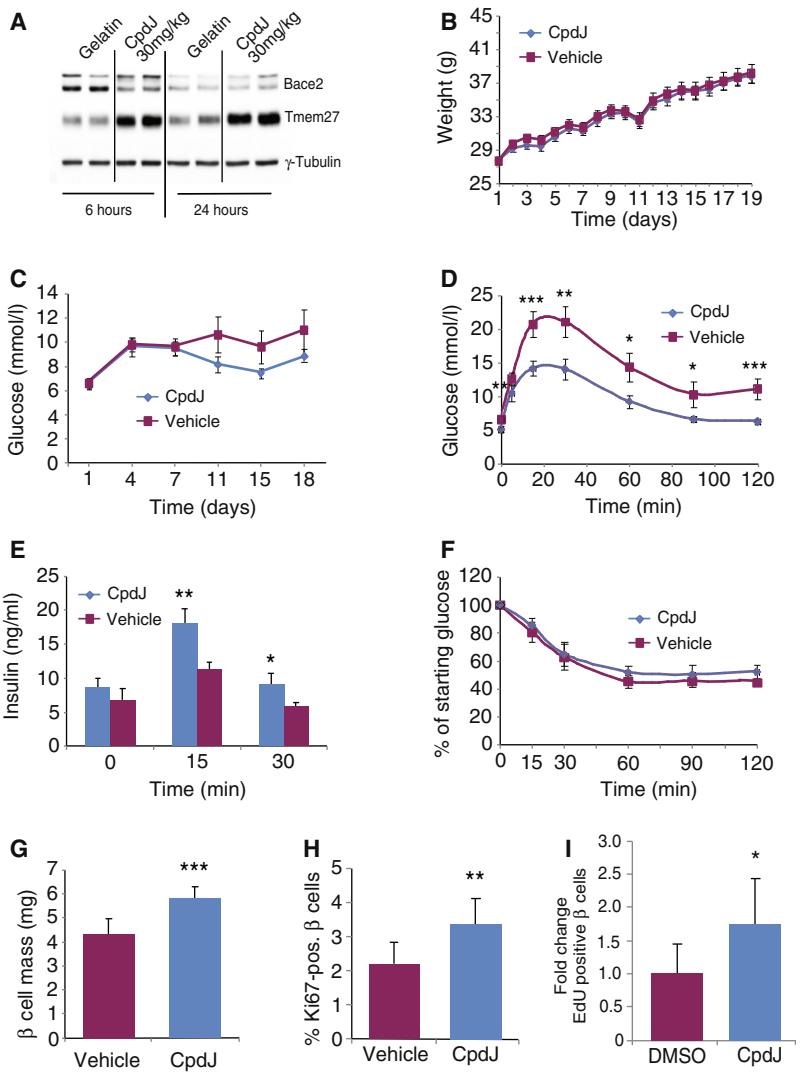

Figure 7. Improved Glucose Tolerance and Increased β Cell Mass in *ob/ob* Mice Treated with 30 mg/kg CpdJ

(A) Western blot for Tmem27 and Bace2 protein of *ob/ob* islets isolated 6 or 24 hr after a single i.p. injection in 5-week-old mice with vehicle or 30 mg/kg CpdJ. Note that by densitrometric analysis the ratio of Bace2 zymogen to mature Bace2 is increased 1.35-fold upon CpdJ after 6 hr, and 1.15-fold after 24 hr, compared to vehicle treatment.

(B) Body weight of *ob/ob* mice treated with 30 mg/kg CpdJ or vehicle from week 5 of age (n = 11).

(C) Blood glucose levels of *ob/ob* mice treated with 30 mg/kg CpdJ or vehicle after a 6 hr fast in the course of 18 days (n = 11).

(D) Blood glucose levels before (0 min, after 12 hr fast) and after an i.p. glucose injection (1 g/kg body weight) in *ob/ob* mice treated with 30 mg/kg CpdJ or vehicle for 11 days (n = 11).

(E) Serum insulin levels after a 12 hr fast (0 min) and an i.p. glucose injection (1g/kg body weight) in *ob/ob* mice treated with 30 mg/kg CpdJ or vehicle for 11 days (n = 11).

(F) ITT in *ob/ob* mice treated with either 30 mg/kg CpdJ or vehicle for 15 days, using 2U insulin/kg body weight (n = 6).

(G) Pancreatic β cell mass of *ob/ob* mice treated with 30 mg/kg CpdJ or vehicle for 20 days (n = 4). Mass was calculated by multiplying the fraction of β cell-positive surface area by pancreatic wet weight.

(H) Percentage of Ki67-positive β cell nuclei in pancreata of *ob/ob* mice treated with 30 mg/kg CpdJ or vehicle for 20 days (n = 6).

(I) Fold change of EdU-positive β cells in dispersed *ob/ob* islets from 5-week-old animals after 60 hr incubation in the presence of 10 μM EdU and 100 nM CpdJ compared to DMSO (n = 4). At least 3000 β cells were counted per animal. Percentage of EdU-positive cells was 0.5%–1.5%. Data shown in (B)–(H) were obtained from the same set of animals and represent means ± SD. *p ≤ 0.05; **p ≤ 0.01; ***p ≤ 0.001.

synergistically contribute to the regulation of β cell mass and function.

Although Bace2 inhibition leads to a rapid stabilization of Tmem27 and a measurable effect on β cell proliferation within days, we did not observe an acute effect on murine β cell insulin secretion. This indicates that long-term reprogramming of the murine islet may be required for the manifestation of the alteration in β cell function, but the exact mechanism(s) and time course remain to be elucidated—possibly by novel Bace2 target identification. Although the preceding β cell proliferation and only subsequent manifestation of enhanced β cell function upon Bace2 inhibition are not necessarily causally linked, it seems plausible that augmented β cell mass will contribute to the improved β cell function.

In human islets, CpdJ had no significant effect on β cell proliferation under our experimental conditions, although Bace2 could be targeted, Tmem27 stabilized, and GSIS augmented on a shorter timescale. Such species-to-species variations in β cell properties have been observed previously (Maechler et al., 2002), especially the resilience of human β cells to proliferative stimuli in vitro (Parnaud et al., 2008). Our data do suggest that the basic Bace2-Tmem27 axis is conserved and that Bace2 inhibition may lead to improved human β cell function. One major limitation of such studies is the lack of in vivo data in humans. However, given the more advanced Bace1 inhibitor programs in the Alzheimer's disease research field, our observations strongly encourage the measurement of glycemic parameters during such studies. While the development of

(G) In vitro insulin secretion of isolated murine islets from 12-week-old mice (four batches of 25 islets per condition) incubated with the indicated glucose or human GLP-1 (7-36) concentration. Islets were treated with 100 nM CpdJ or DMSO 8 hr prior to and throughout assay.

(H) Western blot for hTmem27, and hBace2 in CL of human islets derived from two donors after treatment with 200 nM of CpdJ for 72 hr. Data represent means ± SD. *p ≤ 0.05; **p ≤ 0.01; ***p ≤ 0.001.

Bace1-selective compounds has been challenging so far, our studies suggest that nonselective inhibitors may even be desirable in attempts to prevent Alzheimer's, since type 1 and type 2 diabetes (Park, 2011) represent major risk factors to developing this neurodegenerative disease.

EXPERIMENTAL PROCEDURES

Experimental Animals

All animals were maintained in a pathogen-free facility at the Institute for Molecular Systems Biology, ETH Zürich. The animals were kept on a 12 hr light/dark cycle and fed a standard rodent chow diet (Kliba-Nafag) from 3 weeks of age.

Human Islets

Human islets were obtained through the Juvenile Diabetes Research Foundation (JDRF) Islet Distribution Program. The use of human material was approved through the ETH ethical committee.

Vectors

The hTmem27-encoding vectors were described previously (Akpinar et al., 2005). The C-terminal deletion mutant of hTmem27 was generated by deleting amino acid residues 171–222 using a PCR approach. The point mutations in Bace2 were introduced using the QuickChange II XL site-directed mutagenesis kit (Stratagene). The Bace2ΔE6 construct was obtained by deleting exon 6 using a PCR approach.

Cell Culture

MIN6 cells were maintained in DMEM containing 25 mM glucose, 15% FBS, and 55 μM β-mercaptoethanol. HEK293 cells were grown on DMEM with 25 mM glucose and 10% FBS. Isolated murine islets were cultured in RPMI with 11 mM glucose and 10% FBS, and human islets in CMRL with 5.6 mM glucose and 10% FBS. For shedding experiments, the medium was exchanged to Opti-MEM (Invitrogen).

RNA Interference Screen

SiRNAs against Tmem27 were used as described previously (Akpinar et al., 2005). SiRNA smart pools containing four different sequences targeting each protease were purchased from Dharmacon (see the Supplemental Experimental Procedures, Table S3). MIN6 cells were grown to 30% confluency and electroporated with 100 pmol siRNA/10^6 cells in AMAXA nucleofector V solution using AMAXA single cuvette electroporator and program G-016 (available online at http://www.amaxa.com/). Cells were plated in 6-well plates, and 12 hr after electroporation the medium was exchanged to Opti-MEM for another 24 hr.

Transient Transfection with Plasmids

MIN6 cells were transfected with 5 μg DNA/10^6 cells either by electroporation (see above) or by using Lipofectamine 2000 (Invitrogen). HEK293 cells were transfected with 1.5 μg DNA/10^6 cells using Fugene 6 (Roche) according to the manufacturer's protocol.

In Vitro Protease Inhibition

MIN6 cells were incubated with 100 μM of the BIOMOL inhibitors for 4 hr and indicated doses of Cpd A, B, C, D, and J for 24–48 hr. DAPT was used at 1–10 μM for no longer than 16 hr. Isolated islets were incubated with 100 or 200 nM CpdJ for an indicated period of time.

In Vivo Administration of CpdJ

Mice were i.p. injected with 30 mg/kg or 100 mg/kg body weight of a 15 mg/ml or 50 mg/ml solution of CpdJ in gelatin or vehicle (gelatin).

Statistical Analysis

All values are described as mean ± standard deviation (SD). Statistical significance was determined with a Student's t test, rejecting the null hypothesis at $p = 0.05$, with the exception of the analysis of the MIN6 proliferation assays, which were evaluated by one-way ANOVA followed by Dunnett's post hoc test.

SUPPLEMENTAL INFORMATION

Supplemental Information includes six figures, three tables, Supplemental Experimental Procedures, and Supplemental References and can be found with this article online at doi:10.1016/j.cmet.2011.06.018.

ACKNOWLEDGMENTS

This work was in part sponsored by the JDRF International and by F. Hoffmann-La Roche. We thank P. Salvioni, A. Benardeau, W. Riboulet, S. Uhles, M. Brecheisen, S. Sewing, and T. Lavé for helpful discussions and technical expertise. We thank P. Halban for generously providing the 804G conditioned medium for the islet proliferation assays.

Received: March 9, 2011
Revised: May 11, 2011
Accepted: June 22, 2011
Published: September 6, 2011

REFERENCES

Akpinar, P., Kuwajima, S., Krutzfeldt, J., and Stoffel, M. (2005). Tmem27: a cleaved and shed plasma membrane protein that stimulates pancreatic beta cell proliferation. Cell Metab. *2*, 385–397.

Altirriba, J., Gasa, R., Casas, S., Ramirez-Bajo, M.J., Ros, S., Gutierrez-Dalmau, A., Ruiz de Villa, M.C., Barbera, A., and Gomis, R. (2010). The role of transmembrane protein 27 (TMEM27) in islet physiology and its potential use as a beta cell mass biomarker. Diabetologia *53*, 1406–1414.

Bennett, B.D., Babu-Khan, S., Loeloff, R., Louis, J.C., Curran, E., Citron, M., and Vassar, R. (2000). Expression analysis of BACE2 in brain and peripheral tissues. J. Biol. Chem. *275*, 20647–20651.

Bettegazzi, B., Mihailovich, M., Di Cesare, A., Consonni, A., Macco, R., Pelizzoni, I., Codazzi, F., Grohovaz, F., and Zacchetti, D. (2010). beta-Secretase activity in rat astrocytes: translational block of BACE1 and modulation of BACE2 expression. Eur. J. Neurosci. *33*, 236–243.

Cavallaro, U., and Dejana, E. (2011). Adhesion molecule signalling: not always a sticky business. Nat. Rev. Mol. Cell Biol. *12*, 189–197.

Danilczyk, U., Sarao, R., Remy, C., Benabbas, C., Stange, G., Richter, A., Arya, S., Pospisilik, J.A., Singer, D., Camargo, S.M., et al. (2006). Essential role for collectrin in renal amino acid transport. Nature *444*, 1088–1091.

Dominguez, D., Tournoy, J., Hartmann, D., Huth, T., Cryns, K., Deforce, S., Serneels, L., Camacho, I.E., Marjaux, E., Craessaerts, K., et al. (2005). Phenotypic and biochemical analyses of BACE1- and BACE2-deficient mice. J. Biol. Chem. *280*, 30797–30806.

Donath, M.Y., and Halban, P.A. (2004). Decreased beta-cell mass in diabetes: significance, mechanisms and therapeutic implications. Diabetologia *47*, 581–589.

Efrat, S. (2008). Ex-vivo expansion of adult human pancreatic beta-cells. Rev. Diabet. Stud. *5*, 116–122.

Farzan, M., Schnitzler, C.E., Vasilieva, N., Leung, D., and Choe, H. (2000). BACE2, a beta-secretase homolog, cleaves at the beta site and within the amyloid-beta region of the amyloid-beta precursor protein. Proc. Natl. Acad. Sci. USA *97*, 9712–9717.

Finzi, G., Franzi, F., Placidi, C., Acquati, F., Palumbo, E., Russo, A., Taramelli, R., Sessa, F., and La Rosa, S. (2008). BACE2 is stored in secretory granules of mouse and rat pancreatic beta cells. Ultrastruct. Pathol. *32*, 246–251.

Fluhrer, R., Capell, A., Westmeyer, G., Willem, M., Hartung, B., Condron, M.M., Teplow, D.B., Haass, C., and Walter, J. (2002). A non-amyloidogenic function of BACE-2 in the secretory pathway. J. Neurochem. *81*, 1011–1020.

Francis, R., McGrath, G., Zhang, J., Ruddy, D.A., Sym, M., Apfeld, J., Nicoll, M., Maxwell, M., Hai, B., Ellis, M.C., et al. (2002). aph-1 and pen-2 are required for Notch pathway signaling, gamma-secretase cleavage of betaAPP, and presenilin protein accumulation. Dev. Cell *3*, 85–97.

Fukui, K., Yang, Q., Cao, Y., Takahashi, N., Hatakeyama, H., Wang, H., Wada, J., Zhang, Y., Marselli, L., Nammo, T., et al. (2005). The HNF-1 target collectrin

controls insulin exocytosis by SNARE complex formation. Cell Metab. *2*, 373–384.

Gandhi, S., Refolo, L.M., and Sambamurti, K. (2004). Amyloid precursor protein compartmentalization restricts beta-amyloid production: therapeutic targets based on BACE compartmentalization. J. Mol. Neurosci. *24*, 137–143.

Gruninger-Leitch, F., Schlatter, D., Kung, E., Nelbock, P., and Dobeli, H. (2002). Substrate and inhibitor profile of BACE (beta-secretase) and comparison with other mammalian aspartic proteases. J. Biol. Chem. *277*, 4687–4693.

Han, G.C., Ko, S.K., Sung, J.H., and Chung, S.H. (2007). Compound K enhances insulin secretion with beneficial metabolic effects in db/db mice. J. Agric. Food Chem. *55*, 10641–10648.

Hemming, M.L., Elias, J.E., Gygi, S.P., and Selkoe, D.J. (2009). Identification of beta-secretase (BACE1) substrates using quantitative proteomics. PLoS ONE *4*, e8477. 10.1371/journal.pone.0008477.

Hussain, I., Powell, D.J., Howlett, D.R., Chapman, G.A., Gilmour, L., Murdock, P.R., Tew, D.G., Meek, T.D., Chapman, C., Schneider, K., et al. (2000). ASP1 (BACE2) cleaves the amyloid precursor protein at the beta-secretase site. Mol. Cell. Neurosci. *16*, 609–619.

Hussain, I., Christie, G., Schneider, K., Moore, S., and Dingwall, C. (2001). Prodomain processing of Asp1 (BACE2) is autocatalytic. J. Biol. Chem. *276*, 23322–23328.

Kahn, S.E., Hull, R.L., and Utzschneider, K.M. (2006). Mechanisms linking obesity to insulin resistance and type 2 diabetes. Nature *444*, 840–846.

Kim, Y.T., Downs, D., Wu, S., Dashti, A., Pan, Y., Zhai, P., Wang, X., Zhang, X.C., and Lin, X. (2002). Enzymic properties of recombinant BACE2. Eur. J. Biochem. *269*, 5668–5677.

Kuhn, P.H., Marjaux, E., Imhof, A., De Strooper, B., Haass, C., and Lichtenthaler, S.F. (2007). Regulated intramembrane proteolysis of the interleukin-1 receptor II by alpha-, beta-, and gamma-secretase. J. Biol. Chem. *282*, 11982–11995.

Maechler, P., Gjinovci, A., and Wollheim, C.B. (2002). Implication of glutamate in the kinetics of insulin secretion in rat and mouse perfused pancreas. Diabetes *51* (*Suppl. 1*), S99–S102.

Malakauskas, S.M., Kourany, W.M., Zhang, X.Y., Lu, D., Stevens, R.D., Koves, T.R., Hohmeier, H.E., Muoio, D.M., Newgard, C.B., and Le, T.H. (2009). Increased insulin sensitivity in mice lacking collectrin, a downstream target of HNF-1alpha. Mol. Endocrinol. *23*, 881–892.

Malakauskas, S.M., Quan, H., Fields, T.A., McCall, S.J., Yu, M.J., Kourany, W.M., Frey, C.W., and Le, T.H. (2007). Aminoaciduria and altered renal expression of luminal amino acid transporters in mice lacking novel gene collectrin. Am. J. Physiol. Renal Physiol. *292*, F533–F544.

Park, S.A. (2011). A common pathogenic mechanism linking type-2 diabetes and Alzheimer's disease: evidence from animal models. J. Clin. Neurol. *7*, 10–18.

Parnaud, G., Bosco, D., Berney, T., Pattou, F., Kerr-Conte, J., Donath, M.Y., Bruun, C., Mandrup-Poulsen, T., Billestrup, N., and Halban, P.A. (2008). Proliferation of sorted human and rat beta cells. Diabetologia *51*, 91–100.

Roe, M.W., Philipson, L.H., Frangakis, C.J., Kuznetsov, A., Mertz, R.J., Lancaster, M.E., Spencer, B., Worley, J.F., 3rd, and Dukes, I.D. (1994). Defective glucose-dependent endoplasmic reticulum Ca2+ sequestration in diabetic mouse islets of Langerhans. J. Biol. Chem. *269*, 18279–18282.

Shih, D.Q., Screenan, S., Munoz, K.N., Philipson, L., Pontoglio, M., Yaniv, M., Polonsky, K.S., and Stoffel, M. (2001). Loss of HNF-1alpha function in mice leads to abnormal expression of genes involved in pancreatic islet development and metabolism. Diabetes *50*, 2472–2480.

Sun, X., He, G., and Song, W. (2006). BACE2, as a novel APP theta-secretase, is not responsible for the pathogenesis of Alzheimer's disease in Down syndrome. FASEB J. *20*, 1369–1376.

Turner, R.T., 3rd, Koelsch, G., Hong, L., Castanheira, P., Ermolieff, J., Ghosh, A.K., and Tang, J. (2001). Subsite specificity of memapsin 2 (beta-secretase): implications for inhibitor design. Biochemistry *40*, 10001–10006.

Turner, R.T., 3rd, Loy, J.A., Nguyen, C., Devasamudram, T., Ghosh, A.K., Koelsch, G., and Tang, J. (2002). Specificity of memapsin 1 and its implications on the design of memapsin 2 (beta-secretase) inhibitor selectivity. Biochemistry *41*, 8742–8746.

Walter, J. (2006). Control of amyloid-beta-peptide generation by subcellular trafficking of the beta-amyloid precursor protein and beta-secretase. Neurodegener. Dis. *3*, 247–254.

Winzell, M.S., Wulff, E.M., Olsen, G.S., Sauerberg, P., Gotfredsen, C.F., and Ahren, B. (2009). Improved insulin sensitivity and islet function after PPARdelta activation in diabetic db/db mice. Eur. J. Pharmacol. *626*, 297–305.

Wollscheid, B., Bausch-Fluck, D., Henderson, C., O'Brien, R., Bibel, M., Schiess, R., Aebersold, R., and Watts, J.D. (2009). Mass-spectrometric identification and relative quantification of N-linked cell surface glycoproteins. Nat. Biotechnol. *27*, 378–386.

Yan, R., Munzner, J.B., Shuck, M.E., and Bienkowski, M.J. (2001). BACE2 functions as an alternative alpha-secretase in cells. J. Biol. Chem. *276*, 34019–34027.

Zhang, H., Wada, J., Hida, K., Tsuchiyama, Y., Hiragushi, K., Shikata, K., Wang, H., Lin, S., Kanwar, Y.S., and Makino, H. (2001). Collectrin, a collecting duct-specific transmembrane glycoprotein, is a novel homolog of ACE2 and is developmentally regulated in embryonic kidneys. J. Biol. Chem. *276*, 17132–17139.

Zhang, Y., Wada, J., Yasuhara, A., Iseda, I., Eguchi, J., Fukui, K., Yang, Q., Yamagata, K., Hiesberger, T., Igarashi, P., et al. (2007). The role for HNF-1beta-targeted collectrin in maintenance of primary cilia and cell polarity in collecting duct cells. PLoS ONE *2*, e414. 10.1371/journal.pone.0000414.

Zhao, B., Yu, M., Neitzel, M., Marugg, J., Jagodzinski, J., Lee, M., Hu, K., Schenk, D., Yednock, T., and Basi, G. (2008). Identification of gamma-secretase inhibitor potency determinants on presenilin. J. Biol. Chem. *283*, 2927–2938.